

See discussions, stats, and author profiles for this publication at: <https://www.researchgate.net/publication/221868937>

# [F-18]Fluoro-Deoxy-Glucose Folate: A Novel PET Radiotracer with Improved in Vivo Properties for Folate Receptor Targeting

ARTICLE in BIOCONJUGATE CHEMISTRY · FEBRUARY 2012

Impact Factor: 4.51 · DOI: 10.1021/bc200660z · Source: PubMed

CITATIONS

24

READS

48

## 7 AUTHORS, INCLUDING:



[Josefine Reber](#)

Paul Scherrer Institut

11 PUBLICATIONS 73 CITATIONS

SEE PROFILE



[Adrienne Müller Herde](#)

ETH Zurich

46 PUBLICATIONS 776 CITATIONS

SEE PROFILE



[Stefanie D Krämer](#)

ETH Zurich

100 PUBLICATIONS 1,646 CITATIONS

SEE PROFILE



[Simon Ametamey](#)

ETH Zurich

176 PUBLICATIONS 3,206 CITATIONS

SEE PROFILE

## [<sup>18</sup>F]Fluoro-Deoxy-Glucose Folate: A Novel PET Radiotracer with Improved in Vivo Properties for Folate Receptor Targeting

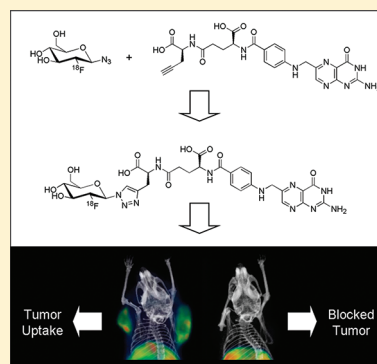
Cindy R. Fischer,<sup>†</sup> Cristina Müller,<sup>‡</sup> Josefine Reber,<sup>‡</sup> Adrienne Müller,<sup>†</sup> Stefanie D. Krämer,<sup>†</sup> Simon M. Ametamey,<sup>†</sup> and Roger Schibli<sup>\*,†,‡</sup>

<sup>†</sup>Center for Radiopharmaceutical Sciences of ETH, PSI and USZ, Institute of Pharmaceutical Sciences, ETH Zurich, Zurich, Switzerland

<sup>‡</sup>Center for Radiopharmaceutical Sciences of ETH, PSI and USZ, Paul Scherrer Institute, Villigen-PSI, Switzerland

**ABSTRACT:** The folate receptor (FR) is upregulated in various cancer types (FR- $\alpha$  isoform) and in activated macrophages (FR- $\beta$  isoform) which are involved in inflammatory and autoimmune diseases, but its expression in healthy tissues and organs is highly restricted to only a few sites (e.g. kidneys). Therefore, the FR is a promising target for imaging and therapy of cancer and inflammation using folate-based radiopharmaceuticals. Herein, we report the synthesis and evaluation of a novel folic acid conjugate with improved properties suitable for positron emission tomography (PET).

[<sup>18</sup>F]-fluoro-deoxy-glucose folate ([<sup>18</sup>F]3) was synthesized based on the click chemistry approach using 2-deoxy-2-[<sup>18</sup>F]fluoroglucopyranosyl azide and a folate alkyne derivative. The novel radiotracer [<sup>18</sup>F]3 was produced in good radiochemical yields (25% d.c.) and high specific radioactivity (90 GBq/ $\mu$ mol). Compared to previously published <sup>18</sup>F-folic acid derivatives, an increase in hydrophilicity was achieved by using a glucose entity as a prosthetic group. Biodistribution and PET imaging studies in KB tumor-bearing mice showed a high and specific uptake of the radiotracer in FR-positive tumors ( $10.03 \pm 1.12\%$  ID/g, 60 min p.i.) and kidneys ( $42.94 \pm 2.04\%$  ID/g, 60 min p.i.). FR-unspecific accumulation of radioactivity was only found in the liver ( $9.49 \pm 1.13\%$  ID/g, 60 min p.i.) and gallbladder ( $17.59 \pm 7.22\%$  ID/g, 60 min p.i.). No radiometabolites were detected in blood, urine, and liver tissue up to 30 min after injection of [<sup>18</sup>F]3. [<sup>18</sup>F]-fluoro-deoxy-glucose-folate ([<sup>18</sup>F]3) is thus a promising PET radioligand for imaging FR-positive tumors.



### INTRODUCTION

The folate receptor (FR) is a membrane-anchored protein which binds the vitamin folic acid with high affinity ( $K_D \sim 10^{-9}$  M). Binding induces internalization via endocytosis. Upregulation of the FR was identified in various cancer types (FR- $\alpha$  isoform) and activated macrophages (FR- $\beta$  isoform), which are involved in inflammatory and autoimmune diseases.<sup>1,2</sup> The fact that the expression of the FR in healthy tissues is limited to only a few sites (kidneys, choroid plexus, lungs, and placenta) makes this receptor a relevant target for imaging and therapy of cancer and inflammation.<sup>3,4</sup>

A number of folate-based radiopharmaceuticals have been developed and preclinically evaluated as diagnostic tools for positron emission tomography (PET) and single photon emission tomography (SPECT) of FR-positive cancer and inflammatory diseases.<sup>5–8</sup> So far, <sup>99m</sup>Tc-EC20 is the only folate-based radiotracer currently used in the clinics.<sup>9</sup> This SPECT tracer is used for identification and selection of patients with FR-positive tumors who could potentially benefit from FR-targeted therapies such as, e.g., the application of folic acid targeted chemotherapeutics<sup>10,11</sup> or FR- $\alpha$  targeted antibodies.<sup>12</sup> Furthermore, <sup>99m</sup>Tc-EC20 has been used for detection of active inflammation in patients with rheumatoid arthritis or osteoarthritis.<sup>6,13</sup> FR-targeted therapies for the treatment of rheumatoid arthritis, based on folic acid conjugates of anti-

inflammatory chemotherapeutics,<sup>14</sup> folate-targeted hapten immunotherapy,<sup>15</sup> or FR- $\beta$  targeted antibodies,<sup>16</sup> are currently under evaluation for clinical use.

However, for the purposes mentioned above a folate radiotracer for PET imaging would be superior since PET is a more accurate nuclear imaging technology than SPECT.<sup>17</sup> The high spatial resolution and high sensitivity which can be achieved by PET would allow detection of marginal accumulation of radioactivity as is expected in the case of small metastases and sites of inflammation. Moreover, the characteristics of the positron decay which establish the basis for a quantitative measurement of accumulated radioactivity<sup>18</sup> would allow determination of FR-expression levels as an important criterion for the application of FR-targeted therapies. Fluorine-18 [<sup>18</sup>F] is the most widely used PET isotope because of its optimal physical decay properties ( $t_{1/2} = 110$  min,  $E_{\beta^+,max} = 0.6$  MeV) that allow multistep syntheses and PET images of high quality. Its relatively long physical half-life allows a distribution of <sup>18</sup>F-labeled radiopharmaceuticals to more distant PET centers.

**Received:** December 9, 2011

**Revised:** February 28, 2012

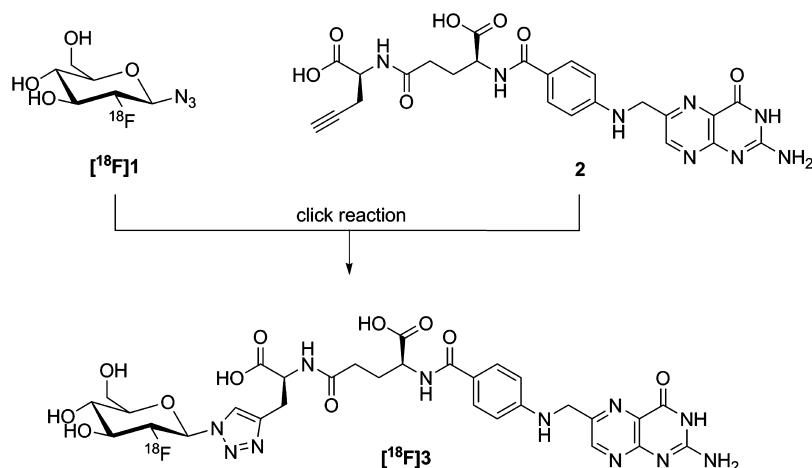


**Figure 1.** Schematic diagram of the radiosynthesis of [ $^{18}\text{F}$ ]fluoro-deoxy-glucose folate ([ $^{18}\text{F}$ ]3).

Several  $^{18}\text{F}$ -based folate tracers have been developed using different labeling approaches. The radioisotope was either introduced by coupling folic acid with a  $^{18}\text{F}$ -radiolabeled prosthetic group<sup>19–21</sup> or by direct radiolabeling of the folic acid molecule.<sup>22</sup> In our group, a  $^{18}\text{F}$ -labeled folate tracer was synthesized that made use of a click chemistry approach ([ $^{18}\text{F}$ ]fluoro-click-folate), which resulted in an excellent overall yield (25–35%).<sup>20</sup> In contrast, adaption of a direct  $^{18}\text{F}$ -labeling strategy where the  $^{18}\text{F}$ -label was introduced at the 2'-position of the 4-amino-benzoyl moiety of folic acid (2'-[ $^{18}\text{F}$ ]fluorofolate) resulted in an only low yield (1–5%).<sup>22</sup> The [ $^{18}\text{F}$ ]fluoro-click-folate tracer revealed unfavorable in vivo distribution characteristics in mice as a consequence of its high overall lipophilicity.<sup>20</sup> However, application of the more hydrophilic 2'-[ $^{18}\text{F}$ ]fluorofolate allowed excellent tumor visualization via PET with only negligible retention of radioactivity in nontargeted tissues and organs.<sup>22</sup> These results suggest a need for a hydrophilic folate radiotracer which can be produced in high radiochemical yields.

The aim of this study was to combine the advantage of the click chemistry approach for the coupling reaction of a  $^{18}\text{F}$ -radiolabeled prosthetic group with the application of a hydrophilic prosthetic group of a well established radiolabeling procedure. Thus, we employed a  $^{18}\text{F}$ -labeled glucose entity as a prosthetic group for coupling to a folate alkyne derivative (Figure 1). This  $^{18}\text{F}$ -labeled glucose prosthetic group was previously described by Maschauer et al. for peptide labeling.<sup>23,24</sup> The novel [ $^{18}\text{F}$ ]fluoro-deoxy-glucose-folate radiotracer was investigated with regard to its in vitro characteristics and in vivo distribution in mice bearing FR-positive tumor xenografts.

## EXPERIMENTAL PROCEDURES

**General.** Reagents and solvents were purchased from Sigma-Aldrich, Merck AG or VWR International AG. All chemicals were used as supplied unless stated otherwise. The  $N^2,N$ -dimethylaminomethylene-10-formylpteroic acid (protected pteric acid, **8**) was generously provided by Merck & Cie (Schaffhausen, Switzerland). Nuclear magnetic resonance spectra were recorded on a Bruker 400 or 500 MHz spectrometer with the corresponding solvent signals as an internal standard. Chemical shifts are reported in parts per million (ppm) relative to tetramethylsilane (0.00 ppm). Values of the coupling constant,  $J$ , are given in hertz (Hz); the following abbreviations are used in this section for the

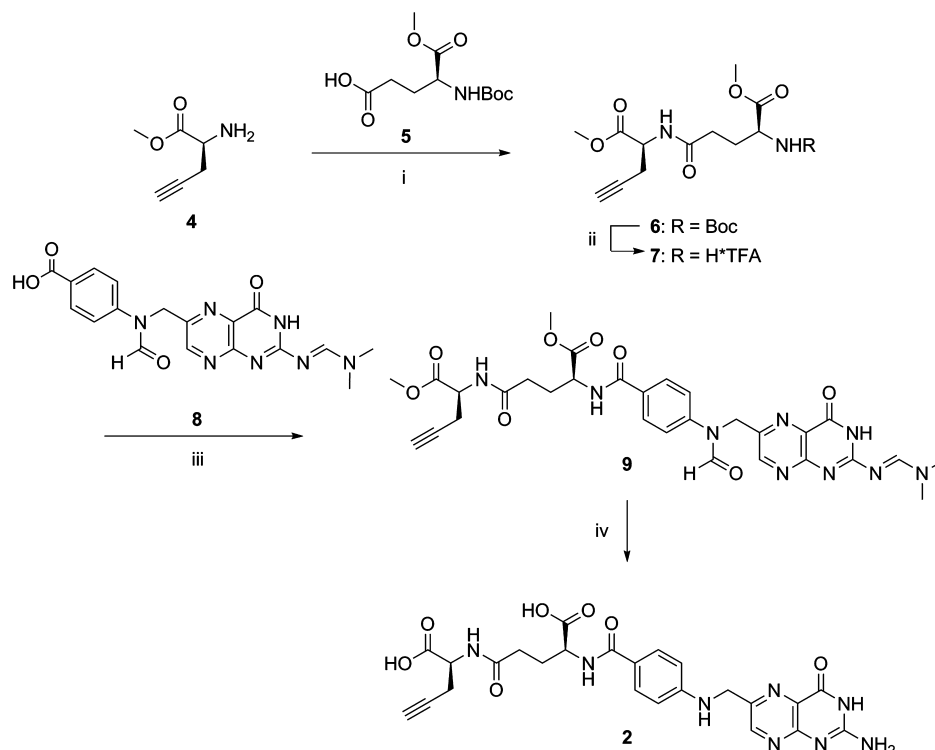
description of  $^1\text{H}$  NMR spectra: singlet (s), doublet (d), triplet (t), quartet (q), multiplet (m), doublet of doublets (dd), and bs (broad singlet). The chemical shifts of complex multiplets are given as the range of their occurrence. For signal assignment, H/D exchange and 2D-NMR experiments (COSY, HSQC) were performed for all new compounds. Low resolution mass spectra (LR-MS) were recorded with a Micromass Quattro micro API LC-ESI and high resolution mass spectra (HR-MS) with a Bruker FTMS 4.7 T BioAPEXII (ESI). Reactions were monitored by thin layer chromatography (TLC, performed on Merck precoated silica gel 60 F-254 aluminum plates) or HPLC.

HPLC was performed on a Merck-Hitachi L-7000 system equipped with a L-7400 tunable absorption detector. Analytical HPLC was performed with a reversed-phase column (Gemini C18, 5  $\mu\text{m}$ , 4.6  $\times$  250 mm, Phenomenex) using 50 mM  $\text{NH}_4\text{HCO}_3$  solution (solvent A) and acetonitrile (solvent B) as a solvent system with a gradient from 0–4 min 100% A, 4–5 min 100–93% A, 5–15 min 93% A, 15–25 min 93–30% A, and 25–30 min 30% A, and a flow rate of 1 mL/min. Semipreparative HPLC was performed with a reversed-phase semipreparative column (Gemini C18, 5  $\mu\text{m}$ , 10  $\times$  250 mm, Phenomenex) at a flow rate of 3 mL/min with 50 mM  $\text{NH}_4\text{HCO}_3$  solution (solvent A) and methanol (solvent B) as the solvent system and a gradient as follows: 0–3 min 100% A, 3–28 min 100–40% A, 28–30 min 40–30% A, and 30–35 min 30% A.

Analytical radio-HPLC was performed on a Merck-Hitachi L-2130 system equipped with a L-2450 diode array detector and a Berthold radiodetector with a reversed-phase column (Gemini C18, 5  $\mu\text{m}$ , 4.6  $\times$  250 mm, Phenomenex) using the above-mentioned gradient for the analytical HPLC.

For the stability studies in vitro and radiometabolites ex vivo, an ultraperformance liquid chromatography (UPLC, Waters) system with an Acquity UPLC BEH C18 column (2.1  $\times$  50 mm, 1.7  $\mu\text{m}$ , Waters) and an attached coincidence detector (FlowStar LBS13, Berthold) was used with 50 mM  $\text{NH}_4\text{HCO}_3$  solution (solvent A) and acetonitrile (solvent B) as solvents and a gradient from 0–0.5 min 100% A, 0.5–3.5 min 100–30% A, and 3.5–3.9 min 30% A at a flow rate of 0.5 mL/min.

Semipreparative radio-HPLC was performed on a HPLC system equipped with a Merck-Hitachi L-6200A intelligent pump, a Knauer variable-wavelength ultraviolet detector and an Eberline RM-14 radiodetector. [ $^{18}\text{F}$ ]fluoro-deoxy-glucose folate

Scheme 1. Synthesis of Folate Alkyne (2)<sup>a</sup>


<sup>a</sup>(i) HBTU, Et<sub>3</sub>N, DMF, 0 °C to rt, 20 h, 82%; (ii) TFA/CH<sub>2</sub>Cl<sub>2</sub> (1:9), rt, 5 h, quant.; (iii) HBTU, Et<sub>3</sub>N, DMF, 0 °C to rt, 6 h; (iv) aq. NaOH (1 M), rt, 15 h, 38% (over 2 steps).

([<sup>18</sup>F]3) was purified on a reversed-phase column (Gemini C18, 5  $\mu$ m, 250  $\times$  10 mm, Phenomenex) using an isocratic solvent system of 5% ethanol in 50 mM NaH<sub>2</sub>PO<sub>4</sub>/Na<sub>2</sub>HPO<sub>4</sub> Soerensen buffer solution (pH 7.5) at a flow rate of 3 mL/min.

Specific radioactivity was determined from a calibration curve obtained from different concentrations of the nonradioactive reference compound [<sup>19</sup>F]fluoro-deoxy-glucose folate (3).

**Synthesis of Intermediate 7.** To a solution of BocGluOMe (5, 402 mg, 1.54 mmol) in dry DMF (4 mL) and Et<sub>3</sub>N (428  $\mu$ L, 2 equiv), HBTU (700 mg, 1.85 mmol) was added at 0 °C. The mixture was stirred for 30 min at 0 °C. The activated acid was added to a solution of H-Pra-OMe·HCl (4, 205 mg, 1.62 mmol) in dry DMF (4 mL) containing Et<sub>3</sub>N (856  $\mu$ L, 4 equiv) at 0 °C. The mixture was stirred for 1 h at 0 °C, warmed to rt, and stirred overnight. The product was extracted with citric acid (1 M, 50 mL) and ethyl acetate (50 mL), and the organic phase was rinsed with brine, dried over Na<sub>2</sub>SO<sub>4</sub>, and concentrated under reduced pressure. Purification was achieved by flash chromatography on silica gel with CH<sub>2</sub>Cl<sub>2</sub>/MeOH (50:1). Product 6 was obtained as a white solid (467 mg, 82%). <sup>1</sup>H NMR (DMSO-*d*<sub>6</sub>)  $\delta$ /ppm 8.40 (d, 1H, *J* = 7.3 Hz), 7.27 (d, 1H, *J* = 7.7 Hz), 4.45 (q, 1H, *J* = 7.3 Hz), 4.00 (m, 1H), 3.68 (s, 3H), 3.66 (s, 3H), 2.92 (t, 1H, *J* = 2.5 Hz), 2.62 (m, 2H), 2.26 (t, 2H, *J* = 7.6 Hz), 2.04–1.71 (m, 2H), 1.42 (s, 9H); <sup>13</sup>C NMR (DMSO-*d*<sub>6</sub>)  $\delta$ /ppm 173.8, 172.4, 171.8, 156.4, 80.9, 79.1, 74.1, 53.9, 53.0, 52.6, 51.9, 32.2, 29.1, 27.5, 21.9. HR-MS (ES<sup>+</sup>) calculated for C<sub>17</sub>H<sub>27</sub>N<sub>2</sub>O<sub>7</sub>: 371.1813; found, 371.1816.

Boc-protected intermediate 6 (460 mg, 1.24 mmol) was dissolved in CH<sub>2</sub>Cl<sub>2</sub> (4.5 mL), and trifluoroacetic acid (TFA; 0.5 mL) was added. The mixture was left at rt for 5 h and then concentrated under reduced pressure to yield the TFA salt of

amine 7 as a yellow oil (332 mg, quantitative). <sup>1</sup>H NMR (DMSO-*d*<sub>6</sub>)  $\delta$ /ppm 8.56 (d, 1H, *J* = 7.3 Hz), 8.48 (bs, 1H), 4.46 (q, 1H, *J* = 7.3 Hz), 4.10 (bs, 1H), 3.79 (s, 3H), 3.68 (s, 3H), 2.95 (t, 1H, *J* = 2.6 Hz), 2.64 (m, 2H), 2.38 (m, 2H), 2.04 (m, 2H); <sup>13</sup>C NMR (DMSO-*d*<sub>6</sub>)  $\delta$ /ppm 171.9, 171.7, 170.6, 81.0, 74.3, 53.8, 53.0, 52.5, 52.0, 31.1, 26.8, 21.9. HR-MS (ES<sup>+</sup>) calculated for C<sub>12</sub>H<sub>19</sub>N<sub>2</sub>O<sub>5</sub>: 271.1288; found, 271.1298.

**Synthesis of Folate Alkyne (2).** To a suspension of protected pteric acid (8, 246 mg, 0.62 mmol) in dry DMF (2 mL) and Et<sub>3</sub>N (165  $\mu$ L, 2 equiv), HBTU (314 mg, 0.83 mmol) was added at 0 °C. The suspension was stirred for 5 min until a clear orange solution appeared. The resulting solution was added at 0 °C to a solution of amine 7 (TFA salt; 160 mg, 0.59 mmol) in dry DMF (3 mL) containing Et<sub>3</sub>N (165  $\mu$ L, 2 equiv). The clear yellow solution was stirred at 0 °C for 4 h and then allowed to warm to rt and stirred for 2 h. Removal of volatile components under reduced pressure and purification of the residue by flash chromatography on silicagel with CH<sub>2</sub>Cl<sub>2</sub>/MeOH (10:1) provided product 9 as a yellow solid (238 mg, 62%). LR-MS [M + H]<sup>+</sup>: 647.83.

NMR and HPLC indicated partial deprotection of the product; thus, compound 9 was deprotected directly to yield folate alkyne 2 using the procedure described below.

Protected folate alkyne 9 (203 mg, 0.35 mmol) was dissolved in 1 M NaOH (6 mL) and stirred overnight at rt. The aqueous solution was extracted with small amounts of ethyl acetate (3  $\times$  1 mL), and afterward, the pH was adjusted to 8 with 2 M HCl (3 mL). The solution was passed through a reversed-phase cartridge (Sep-Pak C18, 12 cm<sup>3</sup>, 2 g; Waters; preconditioned with MeOH (5 mL) and H<sub>2</sub>O (5 mL)). The cartridge was first washed with H<sub>2</sub>O (3 mL), and then the product was eluted with H<sub>2</sub>O (12 mL). After lyophilization of the product fraction,



the folate alkyne **2** was obtained as a yellow powder (121 mg, 63%, purity according to HPLC >95%).  $^1\text{H}$  NMR ( $\text{D}_2\text{O}/\text{NaOD}$ )  $\delta/\text{ppm}$  8.62 (s, 1H), 7.69 (d, 2H,  $J = 8.8$  Hz), 6.86 (d, 2H,  $J = 8.8$  Hz), 4.63 (s, 2H), 4.37 (q, 1H,  $J = 4.5$  Hz), 4.24 (t, 1H,  $J = 5.7$  Hz), 2.56 (m, 2H), 2.44 (m, 2H), 2.29 (m, 1H), 2.07 (m, 1H). HR-MS ( $\text{ES}^+$ ) calculated for  $\text{C}_{24}\text{H}_{25}\text{N}_8\text{O}_7$ : 537.1841; found, 537.1834.

**Synthesis of [ $^{19}\text{F}$ ]Fluoro-deoxy-glucose Folate (**3**).** The synthesis of 2-deoxy-2-fluoroglucopyranosyl azide (**1**) was prepared according to the procedure described by Maschauer et al.<sup>23</sup> To a solution of folate alkyne (**2**, 10 mg, 19  $\mu\text{mol}$ ) in  $^t\text{BuOH}/\text{H}_2\text{O}$  (1:1, 1 mL) in an Eppendorf tube, 2-deoxy-2-fluoroglucopyranosyl azide (**1**, 11.6 mg, 56  $\mu\text{mol}$ ), 0.1 M  $\text{Cu}(\text{OAc})_2$  solution (0.1 eq., 19  $\mu\text{L}$ ) and 0.1 M sodium ascorbate solution (0.2 eq., 38  $\mu\text{L}$ ) were added. The solution was shaken at rt and 500 rpm for 1 h until complete conversion. The reaction progress was followed by analytical HPLC. For isolation of the product, the mixture was submitted to semipreparative HPLC. The desired fraction was collected and lyophilized to provide product **3** as a yellow powder (7.2 mg, 52%, purity according to HPLC >98%).  $^1\text{H}$  NMR ( $\text{D}_2\text{O}/\text{NaOD}$ )  $\delta/\text{ppm}$  8.74 (s, 1H), 7.98 (s, 1H), 7.61 (d, 2H,  $J = 8.8$  Hz), 6.76 (d, 2H,  $J = 8.8$  Hz), 5.89 (dd, 1H,  $J_1 = 2.6$  Hz,  $J_2 = 9.0$  Hz), 4.91 (t, 1H,  $J = 9.0$  Hz), 4.61 (s, 2H), 4.44 (q, 1H,  $J = 4.7$  Hz), 4.35 (q, 1H,  $J = 4.3$  Hz), 4.02–3.86 (m, 2H), 3.79–3.62 (m, 2H), 3.20 (dd, 1H,  $J_1 = 4.7$  Hz,  $J_2 = 14.8$  Hz), 3.04 (dd, 1H,  $J_1 = 8.4$  Hz,  $J_2 = 14.8$  Hz), 2.37 (m, 2H), 2.17 (m, 1H), 2.01 (m, 1H). HR-MS ( $\text{ES}^+$ ) calculated for  $\text{C}_{30}\text{H}_{35}\text{FN}_{11}\text{O}_{11}$ : 744.2496; found, 744.2508.

**Radiochemistry.** No-carrier-added [ $^{18}\text{F}$ ]fluoride was produced via the  $^{18}\text{O}(\text{p},\text{n})^{18}\text{F}$  nuclear reaction at a Cyclone 18/9 cyclotron (IBA) by irradiation of enriched  $^{18}\text{O}$ -water. [ $^{18}\text{F}$ ]fluoride was immobilized on an anion-exchange cartridge (QMA Light; Waters; preconditioned with 0.5 M  $\text{K}_2\text{CO}_3$ -solution (5 mL) and  $\text{H}_2\text{O}$  (5–10 mL)) and eluted with a solution of Kryptofix  $\text{K}_{2.2.2}$  (5 mg) and  $\text{K}_2\text{CO}_3$  (1 mg) in acetonitrile (1.4 mL) and water (0.6 mL) into a 10 mL sealed reaction vessel. The [ $^{18}\text{F}$ ]fluoride (ca. 50–55 GBq) was dried by azeotropic distillation of acetonitrile at 110  $^\circ\text{C}$  under vacuum with a stream of nitrogen. The azeotropic drying process was repeated 3 times with 1 mL of acetonitrile.

The synthesis of 2-deoxy-2-[ $^{18}\text{F}$ ]fluoroglucopyranosyl azide ([ $^{18}\text{F}$ ]**1**) was prepared according to the procedure described by Maschauer et al.<sup>23</sup>

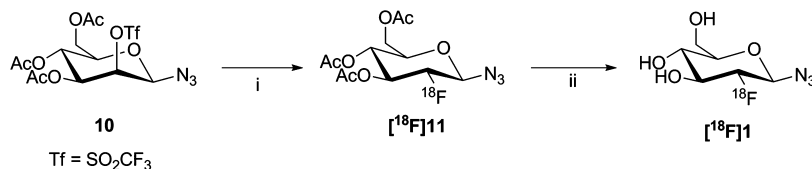
To the dried [ $^{18}\text{F}$ ]fluoride-cryptate complex, the precursor solution of 3,4,6-tri-*O*-acetyl-2-*O*-trifluoromethanesulfonyl- $\beta$ -D-mannopyranosyl azide (**10**, 3.0 mg, 6.5  $\mu\text{mol}$ ) in anhydrous acetonitrile (300  $\mu\text{L}$ ) was added. The mixture was stirred for 5 min at 80  $^\circ\text{C}$ . After 5 min of cooling, 8 mL of water was added to the reactive vial. The mixture was passed through a reversed-phase cartridge (Sep-Pak C18 Plus; Waters; preconditioned with MeOH (5 mL) and  $\text{H}_2\text{O}$  (5 mL)). The cartridge was washed with 5 mL of water, then  $^{18}\text{F}$ -labeled protected intermediate, 3,4,6-tri-*O*-acetyl-2-deoxy-2-[ $^{18}\text{F}$ ]fluoroglucopyranosyl azide ([ $^{18}\text{F}$ ]**11**) was eluted with 2.0 mL of acetonitrile into another 5 mL sealed reaction vessel and dried under reduced pressure with a stream of nitrogen at 80  $^\circ\text{C}$ . For hydrolysis, sodium hydroxide solution (250  $\mu\text{L}$ , 60 mM) was added, and the mixture was heated to 65  $^\circ\text{C}$  for 5 min. After cooling, the mixture was neutralized with hydrogen chloride solution (250  $\mu\text{L}$ , 60 mM) and directly used for the click reaction without further purification. The deprotected [ $^{18}\text{F}$ ]**1** was transferred into another reaction vessel containing

the folate alkyne **2**, followed by the addition of ethanol (300  $\mu\text{L}$ ),  $\text{Cu}(\text{OAc})_2$  solution (10  $\mu\text{L}$ , 0.1 M), and sodium ascorbate solution (20  $\mu\text{L}$ , 0.1 M). The reaction mixture was stirred at 50  $^\circ\text{C}$  for 15 min, and after the addition of phosphate buffer solution (3 mL, 0.15 M), the mixture was purified by semipreparative radio-HPLC. The product fraction of [ $^{18}\text{F}$ ]**3** was collected and passed through a sterile filter into a sterile, pyrogen-free vial without further formulation.

**Determination of Distribution Coefficient.** The distribution coefficient ( $\log D_{7.4}$ ) was determined by the shake flask method.<sup>25</sup> In brief, [ $^{18}\text{F}$ ]**3** was dissolved in a mixture of phosphate buffer (500  $\mu\text{L}$ , pH 7.4) and *n*-octanol (500  $\mu\text{L}$ ) at 20  $^\circ\text{C}$ . The sample was equilibrated for 15 min in an overhead shaker. The two phases were separated by centrifugation (3 min, 5000 rpm), and 50  $\mu\text{L}$  aliquots each of both phases were analyzed in a  $\gamma$ -counter (Wizard, PerkinElmer). The partition coefficient is expressed as the ratio between the radioactivity concentrations (cpm/mL) of the octanol and the buffer phase. Values represent the mean  $\pm$  standard deviation of eight determinations from two independent experiments.

**Binding Affinity Assays in Vitro.** Binding affinity assays were performed with KB cells derived from human cervical carcinoma (DSMZ ACC136). The cells were cultured in a folate-free culture medium FFRPMI (modified RPMI, without folic acid, vitamin  $\text{B}_{12}$ , and phenol red, Cell Culture Technologies GmbH) supplemented with 10% heat-inactivated fetal calf serum (as the only source of folate), L-glutamine and antibiotics (penicillin/streptomycin/fungizone) at 37  $^\circ\text{C}$  in a humidified atmosphere (5%  $\text{CO}_2$ ). For the binding assay, a cell suspension in FFRPMI medium (no additives, ice-cold, 7000 cells in 240  $\mu\text{L}$ ) was incubated in triplicate with  $^3\text{H}$ -folic acid (0.82 nM, 0.94 TBq/mmol, Moravsek Biochemicals Inc.) and increasing concentrations of the nonradioactive reference compound **3** ( $5.0 \times 10^{-6}$  to  $5.0 \times 10^{-12}$  M) at 4  $^\circ\text{C}$  for 30 min. Nonspecific binding was determined in the presence of excess folic acid ( $10^{-4}$  M). After incubation, the suspension was centrifuged at 1000 rpm and 4  $^\circ\text{C}$  for 5 min, and the supernatant was removed. The cells were lysed by addition of 0.5 mL of 1 N NaOH, stirred on a vortex mixer, and transferred into scintillation tubes containing 5 mL of scintillation cocktail (Ultima Gold; Perkin-Elmer). Radioactivity was measured using a  $\beta$ -counter (LS6500; Beckman), and the inhibitory concentrations of 50% were determined from displacement curves using GraphPad Prism 4.0 software. The relative binding affinity of **3** was determined based on the binding affinity of folic acid which was set to 1.0. A value equal to that of folic acid indicates an equal affinity for the FR, a value lower than 1.0 reflects weaker affinity, and a value higher than 1.0 reflects stronger affinity.<sup>26,27</sup>

**Stability Studies in Vitro.** Stability of [ $^{18}\text{F}$ ]**3** was investigated in human plasma and phosphate buffered saline (PBS) at various incubation times (0–120 min) and 37  $^\circ\text{C}$ . After incubation, plasma proteins were precipitated with ice-cold methanol and centrifuged for 10 min at 13500 rpm and 20  $^\circ\text{C}$ . The samples of [ $^{18}\text{F}$ ]**3** incubated in PBS were diluted with the same volume of methanol. The supernatants of the plasma samples and the PBS samples were analyzed by analytical radio-UPLC. To test metabolism by hepatic microsomal enzymes, [ $^{18}\text{F}$ ]**3** was incubated with human and murine liver microsomes (0.5 mg/mL protein, BD Biosciences). Each sample contained a NADPH regenerating system consisting of solution A containing 31 mM  $\text{NADP}^+$ , 66 mM glucose-6-phosphate, and 66 mM  $\text{MgCl}_2$  in water and solution B containing 40 U/mL

Scheme 2. Radiosynthesis of 2-Deoxy-2-[ $^{18}\text{F}$ ]fluoroglucopyranosyl Azide ( $^{18}\text{F}$ 1)<sup>a</sup>

<sup>a</sup>(i) [ $^{18}\text{F}$ ]KF-K<sub>2.2.2</sub>, MeCN, 80°C, 5 min, 75%; (ii) aq. NaOH (60 mM), 65°C, 5 min, quant.

glucose-6-phosphate dehydrogenase in 5 mM sodium citrate. These two reagents were combined to provide the reducing agent for the reaction with cytochrome P450 (CYP). Control samples were incubated without microsomes or without the NADPH regenerating system. Proteins were precipitated by addition of ice-cold methanol at different time points between 0 and 60 min and centrifugation for 5 min at 13400 rpm. Aliquots of the supernatants were analyzed by radio-UPLC.

**Biodistribution Studies.** All animal experiments complied with Swiss and local laws on animal protection. Female CD-1 nude mice were purchased from Charles River (Germany) and maintained on a folate-deficient rodent diet (Harlan Laboratories, US). After a 5–7 day acclimatization period, 0.1 mL of a KB tumor cell suspension ( $5 \times 10^6$  cells) was inoculated subcutaneously on both shoulders of each mouse. The animal experiments were performed 12 days after tumor cell inoculation. Animals were injected with  $\sim 5$  MBq (0.05–0.07 nmol) of [ $^{18}\text{F}$ ]3 in a volume of 100  $\mu\text{L}$  via a lateral tail vein ( $n = 4$  per time point). Blocking studies ( $n = 3$ ) were performed with excess folic acid dissolved in PBS (100  $\mu\text{g}$  in 100  $\mu\text{L}$ ) which was intravenously injected 10 min before the radiotracer injection. Animals were sacrificed at the indicated time points, and organs and tissues were collected and measured in the  $\gamma$ -counter. The incorporated radioactivity was expressed as percentage injected dose [% ID] per gram of tissue.

**PET Imaging Studies.** PET experiments were performed with an eXplore VISTA PET/CT tomograph (GE). Animals were injected with 10–14 MBq (0.15–0.23 nmol) of [ $^{18}\text{F}$ ]3 (100–150  $\mu\text{L}$  per injection) via a lateral tail vein. For blocking studies, the animals received excess folic acid (100  $\mu\text{g}$  in 100  $\mu\text{L}$ ) via intravenous injection 10 min prior to the radiotracer injection. Animals were anesthetized with isoflurane in an air/oxygen mixture and scanned as described previously.<sup>28</sup> The PET scans were acquired from 75 to 105 min p.i. After acquisition, PET data were reconstructed in user-defined time frames. The fused data sets of PET and CT were analyzed with Amira (version 4.0) postprocessing software.

**Metabolite Studies ex Vivo.** For the determination of radiometabolites in vivo, [ $^{18}\text{F}$ ]3 (50–70 MBq; 0.35 nmol–0.49 nmol) was intravenously injected into mice without tumors ( $n = 3$ ). After 5 min, blood samples were withdrawn from the opposite vein, and the animals were sacrificed 30 min after radiotracer injection. Whole blood, liver, and urine were collected. Blood samples were centrifuged at 5000g for 5 min at 4 °C. The proteins of the plasma samples were precipitated by addition of ice-cold methanol followed by centrifugation. The supernatants of the plasma samples and the urine samples were analyzed by radio-UPLC and radio-TLC, respectively. Liver tissue was homogenized in an equal volume of PBS using a PT 1200 C Polytron (Kinematica AG). After centrifugation (5000g, 5 min, 4 °C), the supernatant was cleared from proteins by addition of ice-cold methanol and centrifugation. The super-

natant was analyzed by radio-UPLC and radio-TLC, respectively.

## RESULTS

**Chemistry and Radiochemistry.** The synthesis of folate alkyne 2 was obtained in 4 steps in an overall yield of 31% (Scheme 1). The first step involving the coupling of two commercially available amino acids BocGluOMe (5) and H-Pra-OMe (4) yielded the Boc-protected glutamic acid intermediate 6 in 82% yield. Deprotection of intermediate 6 with TFA afforded amine 7, which was obtained in quantitative yield. Protected folate alkyne 9 was prepared by the coupling of amine 7 with protected pteric acid (8) following a published procedure.<sup>29</sup> The final product folate alkyne 2 was obtained after deprotection of compound 9 and was purified using a reversed-phase cartridge.

The synthesis of the azide component, 2-deoxy-2-fluoroglucopyranosyl azide (1), was accomplished using the procedure described by Maschauer et al.<sup>23</sup> The Cu(I)-catalyzed cycloaddition of azide 1 and folate alkyne 2 was performed in an aqueous system, and after semipreparative HPLC purification the nonradioactive reference compound 3 was achieved in high purity (>98%) and good yield (52%).

The protected glucose azide [ $^{18}\text{F}$ ]11 was obtained by nucleophilic  $^{18}\text{F}$ -substitution of the mannosyl-precursor 10<sup>23</sup> in 75% radiochemical yield after purification by C18 reversed-phase cartridge (Scheme 2). After hydrolysis, crude [ $^{18}\text{F}$ ]1 was neutralized and used for the click reaction without further purification. A complete conversion to [ $^{18}\text{F}$ ]3 was observed by UPLC after 15 min at 50 °C. [ $^{18}\text{F}$ ]3 was purified by reversed-phase semipreparative HPLC. The desired product peak (retention time 20 min) was directly collected into a sterile, pyrogen-free product vial after passing through a sterile filter. The solution was either immediately used for biological applications or diluted with PBS. After an overall synthesis time of 3 h, a maximum activity amount of 1–3 GBq isolated product [ $^{18}\text{F}$ ]fluoro-deoxy-glucose folate ([ $^{18}\text{F}$ ]3) was obtained in decay-corrected radiochemical yields of 5–25%, with a radiochemical purity  $\geq 95\%$  and a specific activity (EOS) of  $90 \pm 38$  GBq/ $\mu\text{mol}$ . [ $^{18}\text{F}$ ]3 was identified by coinjection with its nonradioactive reference compound 3 by analytical HPLC (Figure 2).

**In Vitro Characterization.** The relative binding affinity of the nonradioactive fluoro-deoxy-glucose folate (3) was obtained from three independent experiments and was  $0.63 \pm 0.05$  compared to folic acid which was set to 1.0. The displacement curves of one representative experiment are shown in Figure 3. The log D<sub>7.4</sub> value of [ $^{18}\text{F}$ ]3 was  $-4.2 \pm 0.1$ . Stability studies in human plasma and human and murine liver microsomes revealed no defluorination or radioactive degradation products of [ $^{18}\text{F}$ ]3 within 120 and 60 min, respectively, at 37 °C.

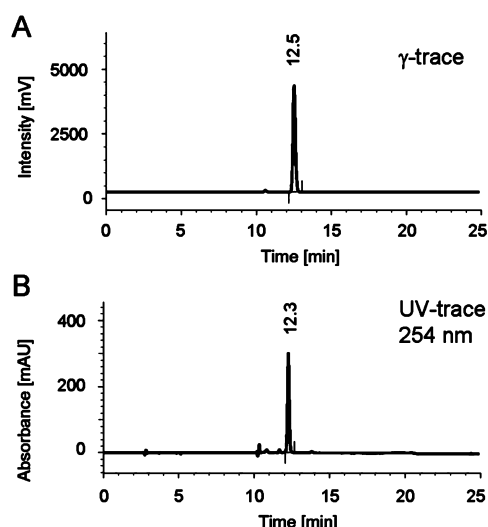


**Figure 2.** HPLC chromatogram of [ $^{18}\text{F}$ ]fluoro-deoxy-glucose folate ([ $^{18}\text{F}$ ]3) (A) with coinjection of the nonradioactive reference compound fluoro-deoxy-glucose folate (3) (B).

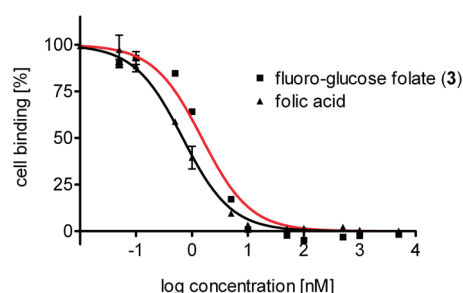


**Figure 3.** Displacement curves of fluoro-deoxy-glucose folate (3) and folic acid using  $^3\text{H}$ -folic acid and human KB tumor cells.

**Biodistribution Studies.** The results of the biodistribution studies are shown in Table 1, including previously reported data of the SPECT tracer  $^{99\text{m}}\text{Tc}$ -EC20.<sup>30</sup> The tumor uptake already reached a value of  $9.61 \pm 1.73\%$  ID/g 30 min after injection of  $\sim 5$  MBq [ $^{18}\text{F}$ ]3, which was similar to the values obtained at 60 min ( $10.03 \pm 1.12\%$  ID/g) and 90 min p.i. ( $9.05 \pm 2.12\%$  ID/g). Radioactivity in the tumor xenografts was reduced by 89% to  $1.19 \pm 1.04\%$  ID/g under blockade conditions. High specific uptake was also found in the kidneys and in the salivary glands, organs with known FR expression.<sup>31</sup> The kidney uptake was high under baseline conditions ( $42.94 \pm 2.04\%$  ID/g; 60 min p.i.) and was reduced to  $3.48 \pm 0.14\%$  ID/g in the blockade group. This means a reduction of 92%, which indicates the high specific binding of [ $^{18}\text{F}$ ]3 to the FR. A similar observation was made in the salivary glands, where the uptake was reduced by 95% from  $5.93 \pm 0.77\%$  ID/g in the baseline group to  $0.30 \pm 0.01\%$  ID/g under blockade conditions. [ $^{18}\text{F}$ ]3 exhibited a fast blood clearance, which resulted in a high tumor-to-blood ratio of  $36.09 \pm 15.37$  at 90 min p.i.. A high nonspecific accumulation was observed in the liver ( $10.82 \pm 1.68\%$  ID/g; 30 min p.i.), which slightly decreased to  $8.37 \pm 1.19\%$  ID/g at 90 min after injection. This uptake leads to tumor-to-liver ratios of  $\sim 1$  at all time points after injection. Furthermore, high radioactivity was found in the gallbladder, urine, and feces, indicating biliary and renal excretion of [ $^{18}\text{F}$ ]3.

**PET Imaging Studies.** The excellent tumor targeting properties of [ $^{18}\text{F}$ ]3 found in biodistribution studies ex vivo were confirmed by PET imaging studies. Both KB tumors on the shoulders and the FR-positive kidneys were clearly imaged under baseline conditions, whereas uptake of [ $^{18}\text{F}$ ]3 in tumors and kidneys was negligible under blockade conditions (Figure 4). Under baseline conditions, high radioactivity was also observed in the liver, gallbladder, and urinary bladder. Uptake of radioactivity in the liver and gallbladder was not reduced under blockade conditions.

**Table 1.** Biodistribution Data of [ $^{18}\text{F}$ ]Fluoro-deoxy-glucose Folate ([ $^{18}\text{F}$ ]3) in Nude Mice Bearing KB Tumor Xenografts<sup>a</sup> in Comparison to the SPECT Tracer  $^{99\text{m}}\text{Tc}$ -EC20<sup>30</sup>

organ or tissue	30 min p.i. ( $n = 4$ )	60 min p.i. ( $n = 4$ )	90 min p.i. ( $n = 4$ )	60 min p.i. blockade <sup>b</sup> ( $n = 3$ )	$^{99\text{m}}\text{Tc}$ -EC20 <sup>30</sup> 60 min p.i. ( $n = 4$ )
% ID/g in					
blood	$0.94 \pm 0.31$	$0.44 \pm 0.09$	$0.25 \pm 0.08$	$1.37 \pm 1.80$	$0.38 \pm 0.12$
brain	$0.38 \pm 0.06$	$0.59 \pm 0.08$	$0.45 \pm 0.07$	$0.04 \pm 0.02$	n.d.
heart	$1.04 \pm 0.14$	$1.15 \pm 0.13$	$0.81 \pm 0.01$	$1.66 \pm 2.05$	n.d.
lungs	$1.18 \pm 0.14$	$0.92 \pm 0.07$	$0.71 \pm 0.12$	$0.46 \pm 0.06$	$1.14 \pm 0.24$
spleen	$0.61 \pm 0.13$	$0.73 \pm 0.21$	$0.60 \pm 0.22$	$0.23 \pm 0.05$	$0.46 \pm 0.12$
liver	$10.82 \pm 1.68$	$9.49 \pm 1.13$	$8.37 \pm 1.19$	$10.00 \pm 3.53$	$5.12 \pm 1.57$
gallbladder	$9.53 \pm 6.01$	$17.59 \pm 7.22$	$27.42 \pm 7.57$	$22.49 \pm 12.25$	n.d.
kidneys	$32.44 \pm 1.84$	$42.94 \pm 2.04$	$27.08 \pm 1.53$	$3.48 \pm 0.14$	$89.18 \pm 10.73$
stomach	$1.27 \pm 0.20$	$1.42 \pm 0.53$	$1.03 \pm 0.01$	$0.33 \pm 0.08$	$1.60 \pm 0.32$
intestine	$1.48 \pm 0.46$	$3.45 \pm 1.61$	$3.69 \pm 0.04$	$4.56 \pm 2.05$	$0.95 \pm 0.38$
feces	$6.56 \pm 4.41$	$10.95 \pm 4.33$	$18.40 \pm 6.83$	$20.48 \pm 0.21$	n.d.
salivary glands	$4.61 \pm 0.44$	$5.93 \pm 0.77$	$4.90 \pm 0.01$	$0.30 \pm 0.01$	$8.08 \pm 2.51$
bone	$0.90 \pm 0.13$	$0.87 \pm 0.05$	$0.72 \pm 0.04$	$0.29 \pm 0.01$	$0.70 \pm 0.18$
muscle	$0.89 \pm 0.15$	$0.69 \pm 0.05$	$0.57 \pm 0.12$	$0.26 \pm 0.04$	$0.73 \pm 0.18$
tumor	$9.61 \pm 1.73$	$10.03 \pm 1.12$	$9.05 \pm 2.12$	$1.19 \pm 1.04$	$11.39 \pm 3.24$
ratios					
tumor/liver	$0.89 \pm 0.14$	$1.06 \pm 0.02$	$1.28 \pm 0.22$	$0.15 \pm 0.16$	$2.28 \pm 0.58$
tumor/kidneys	$0.29 \pm 0.04$	$0.23 \pm 0.04$	$0.34 \pm 0.07$	$0.33 \pm 0.28$	$0.13 \pm 0.04$
tumor/blood	$10.57 \pm 1.65$	$24.10 \pm 7.44$	$36.09 \pm 15.37$	$10.61 \pm 14.77$	$30.09 \pm 3.39$

<sup>a</sup>Mice were injected with  $\sim 5$  MBq ( $0.05$ – $0.07$  nmol) of [ $^{18}\text{F}$ ]3 via the lateral tail vein. <sup>b</sup>In the blockade group, each animal received  $100 \mu\text{g}$  of folic acid in PBS 10 min before the radiotracer injection.



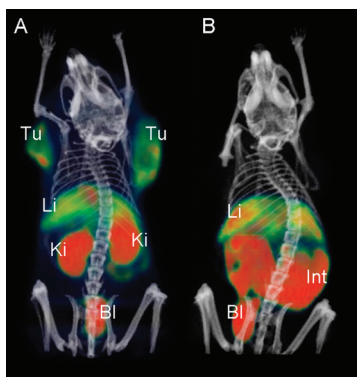


**Figure 4.** Three-dimensional PET/CT images of KB tumor-bearing mice 75–105 min after injection of 10–14 MBq (0.15–0.23 nmol) [ $^{18}\text{F}$ ]fluoro-deoxy-glucose folate ([ $^{18}\text{F}$ ]3): (A) baseline and (B) mouse injected with folic acid prior to radiotracer (Tu, tumor; Li, liver; Ki, kidneys; Bl, urinary bladder; and Int, intestines/feces).

**Metabolite Studies ex Vivo.** To determine whether a radiometabolite was responsible for the liver uptake, ex vivo metabolite studies were carried out to determine potential metabolites. [ $^{18}\text{F}$ ]3 was injected into mice (without tumors). Analysis of plasma, urine, and liver tissue taken 30 min after injection revealed only intact parent compound [ $^{18}\text{F}$ ]3 (Figure 5).

## DISCUSSION

The radiosynthesis of the prosthetic group, 2-deoxy-2- $^{18}\text{F}$ -fluoroglucopyranosyl azide ([ $^{18}\text{F}$ ]1), proceeded in a manner similar to the highly reliable and efficient radiosynthesis of 2-deoxy-2- $^{18}\text{F}$ -fluoroglucose (FDG).<sup>32</sup> For the synthesis of the folate alkyne derivative 2, a fragment coupling strategy was employed. As the main step, a condensation reaction of protected pteric acid and an alkyne substituted glutamic acid part was performed. By combining the click chemistry approach and the well established prosthetic group [ $^{18}\text{F}$ ]1, an efficient procedure was found to synthesize a novel hydrophilic  $^{18}\text{F}$ -labeled folic acid derivative. The radiosynthesis allowed a regiospecific reaction which resulted only in the  $\gamma$ -isomer without the need to perform cumbersome separation of regioisomers.

Compared to our previously published  $^{18}\text{F}$ -labeled folic acid derivatives, [ $^{18}\text{F}$ ]fluoro-deoxy-glucose folate ([ $^{18}\text{F}$ ]3) was produced in excellent radiochemical yields of up to 25% d.c. (up to 3 GBq isolated product) in a total synthesis time of 3 h. The overall time could potentially be reduced by the employment of an automated modular system allowing a standardization of the synthesis and radiolabeling procedure, which will be required for the routine production of the radiotracer. Because of the high selectivity of the 1,3-dipolar cycloaddition in the presence of Cu(I),<sup>33–35</sup> protection of functional groups was not necessary, and thus by application of this strategy, a further deprotection step during the radiosynthesis could be avoided. The use of physiological phosphate buffer as solvent system for the reversed-phase HPLC purification provided the final product [ $^{18}\text{F}$ ]3 in a solution formulated for direct in vitro and in vivo application of the radiotracer.

An increase in hydrophilicity, compared to previously investigated  $^{18}\text{F}$ -labeled folic acid derivatives of our group<sup>19,20,22</sup> was achieved by using a glucose entity as a prosthetic group. The log  $D_{7.4}$  value of  $-4.2 \pm 0.1$  was in a

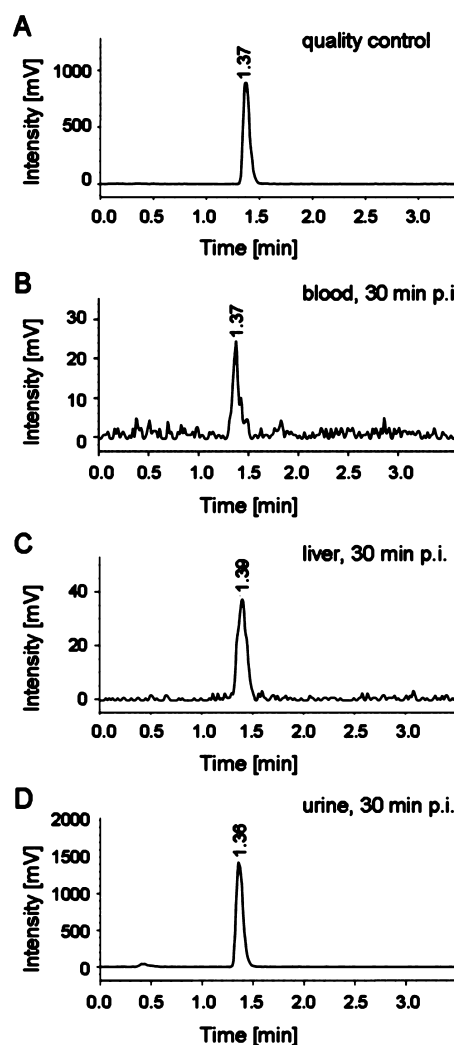


**Figure 5.** Radio-UPLC chromatograms of reference radiotracer [ $^{18}\text{F}$ ]3 (A), blood sample (B), liver tissue (C), and urine sample (D) 30 min after [ $^{18}\text{F}$ ]fluoro-deoxy-glucose folate ([ $^{18}\text{F}$ ]3) injection.

range similar to that of the log  $D_{7.4}$  value of the  $^{111}\text{In}$ -DOTA-folate conjugate, which showed excellent tissue distribution properties, recently published by Müller et al.<sup>36</sup> The presence of only intact radiotracer [ $^{18}\text{F}$ ]3 after 120 min incubation in human plasma or 60 min incubation with human and murine liver microsomes proved its high stability toward hydrolases and oxidoreductases. As expected from these results, the radiotracer was stable in vivo, and no radiometabolites were detected in liver, urine, and blood. Potential release of the  $^{18}\text{F}$ -labeled glucose entity would most probably have resulted in an accumulation of radioactivity in the brain and myocardium, similar to [ $^{18}\text{F}$ ]-FDG.<sup>37</sup> Free [ $^{18}\text{F}$ ]fluoride potentially produced by the defluorination reaction would accumulate in the bones.<sup>38</sup> However, the fact of only background radioactivity in the brain, heart, and bone clearly demonstrated the absence of a glucose-like molecule or [ $^{18}\text{F}$ ]fluoride as potential radiometabolites.

Biodistribution data and PET imaging experiments with [ $^{18}\text{F}$ ]3 confirmed the proposed characteristics of this new radiotracer. [ $^{18}\text{F}$ ]3 showed a comparative tissue distribution to the SPECT tracer  $^{99\text{m}}\text{Tc}$ -EC20 (Table 1). Uptake of [ $^{18}\text{F}$ ]3 in FR-positive KB tumors was high already at 30 min p.i. and remained between 9 and 10% ID/g for the entire study period. Furthermore, a high and specific uptake was found in the



kidneys ( $42.94 \pm 2.04\%$  ID/g; 60 min p.i.), where the FR is expressed on the proximal tubule cells.<sup>4</sup>

Because of the hydrophilic properties of [ $^{18}\text{F}$ ]3, favorable tumor-to-background contrast was achieved shortly after injection and allowed excellent tumor visualization by PET. These results were clearly superior to those obtained with the [ $^{18}\text{F}$ ]fluoro-click-folate, previously synthesized by Ross et al.<sup>20</sup> The lipophilic character of this [ $^{18}\text{F}$ ]fluoro-click-folate and a pronounced hepatobiliary elimination resulted in a high accumulation of radioactivity in the abdominal region. With regard to the tumor-to-background contrast, our novel [ $^{18}\text{F}$ ]fluoro-deoxy-glucose folate ([ $^{18}\text{F}$ ]3) was comparable to 2'-[ $^{18}\text{F}$ ]fluorofolate, where the  $^{18}\text{F}$  label was directly introduced at the 2'-position of the 4-amino-benzoyl moiety in folic acid. The 2'-[ $^{18}\text{F}$ ]fluorofolate also showed a comparable high uptake of  $\sim 9\%$  ID/g (75 min p.i.) in FR-positive KB tumors,<sup>22</sup> but a routine production of that radiotracer would not have been possible due to the unfavorably low radiochemical yield which was achievable.

Despite the hydrophilic character of [ $^{18}\text{F}$ ]3, a relatively high uptake of radioactivity was observed in the liver resulting in a tumor-to-liver ratio of  $\sim 1$ , which was in the same range as that for 2'-[ $^{18}\text{F}$ ]fluorofolate. The SPECT tracer  $^{99\text{m}}\text{Tc}$ -EC20, which was evaluated in the same animal model, showed better tumor-to-liver ratios due to a lower uptake of the radiotracer in the liver.<sup>30</sup> Since liver cells do not express the FR,<sup>4</sup> and only parent radiotracer [ $^{18}\text{F}$ ]3 was detected in liver tissue, a carrier-mediated uptake of the folic acid derivative into the hepatocytes is assumed. These results are in agreement with the findings with the clinically established folate-based radiotracer  $^{99\text{m}}\text{Tc}$ -EC20<sup>9</sup> and correlate well with the observations made by Leamon et al. proposing a liver uptake via promiscuous organic anion transporters.<sup>39</sup>

## CONCLUSIONS

A novel  $^{18}\text{F}$ -labeled folic acid derivative [ $^{18}\text{F}$ ]3 was synthesized using a hydrophilic glucose entity as a radiolabeled prosthetic group to increase the overall hydrophilicity of the radiotracer. The coupling reaction of the [ $^{18}\text{F}$ ]glucose entity and the folic acid precursor was carried out via the well established click chemistry approach. A folate precursor with a mannosyl moiety for a direct radiolabeling could be an alternative strategy. The new [ $^{18}\text{F}$ ]fluoro-deoxy-glucose folate ([ $^{18}\text{F}$ ]3) can be produced by a reliable and high-yielding radiosynthesis and shows high affinity and specificity for the FR, both in vitro and in vivo.

Thus, [ $^{18}\text{F}$ ]fluoro-deoxy-glucose folate is a highly promising  $^{18}\text{F}$ -radiotracer for clinical use as it would be suitable for routine production potentially allowing application in patients for PET imaging of FR-positive cancer and inflammatory diseases.

## AUTHOR INFORMATION

### Corresponding Author

\*Center for Radiopharmaceutical Sciences of ETH, PSI and USZ, Department of Chemistry and Applied Biosciences, ETH Hönggerberg, Wolfgang-Pauli-Strasse 10, CH-8093 Zurich, Switzerland. Phone: +41 44 633 74 64. Fax: +41 44 633 13 67. E-mail: roger.schibli@pharma.ethz.ch.

### Notes

The authors declare no competing financial interest.

## ACKNOWLEDGMENTS

We thank Dr. Linjing Mu, Dr. Selena Milicevic-Sephton, Dr. Alexander Hohn, Dr. Harriet Struthers, Dr. Thomas Betzel, Nadja Romano, Claudia Keller, Petra Wirth, and Dominique Leutwiler for their support and technical assistance.

## REFERENCES

- (1) Low, P. S., Henne, W. A., and Doorneweerd, D. D. (2008) Discovery and development of folic-acid-based receptor targeting for imaging and therapy of cancer and inflammatory diseases. *Acc. Chem. Res.* 41, 120–129.
- (2) Segal, E. I., and Low, P. S. (2008) Tumor detection using folate receptor-targeted imaging agents. *Cancer Metastasis Rev.* 27, 655–664.
- (3) Weitman, S. D., Lark, R. H., Coney, L. R., Fort, D. W., Frasca, V., Zurawski, V. R., and Kamen, B. A. (1992) Distribution of the folate receptor GP38 in normal and malignant cell lines and tissues. *Cancer Res.* 52, 3396–3401.
- (4) Parker, N., Turk, M. J., Westrick, E., Lewis, J. D., Low, P. S., and Leamon, C. P. (2005) Folate receptor expression in carcinomas and normal tissues determined by a quantitative radioligand binding assay. *Anal. Biochem.* 338, 284–293.
- (5) Ke, C. Y., Mathias, C. J., and Green, M. A. (2004) Folate-receptor-targeted radionuclide imaging agents. *Adv. Drug Deliv. Rev.* 56, 1143–1160.
- (6) Paulos, C. M., Turk, M. J., Breur, G. J., and Low, P. S. (2004) Folate receptor-mediated targeting of therapeutic and imaging agents to activated macrophages in rheumatoid arthritis. *Adv. Drug Delivery Rev.* 56, 1205–1217.
- (7) Müller, C., and Schibli, R. (2011) Folic acid conjugates for nuclear imaging of folate receptor-positive cancer. *J. Nucl. Med.* 52, 1–4.
- (8) Müller, C., and Schibli, R. (2011) Folate Receptor-Targeted Radionuclide Imaging Agents, *Targeted Drug Strategies for Cancer and Inflammation* (Jackman, A. L., and Leamon, C. P., Eds.) pp 65–92, Chapter 4, Springer Science, New York.
- (9) Fisher, R. E., Siegel, B. A., Edell, S. L., Oyesiku, N. M., Morgenstern, D. E., Messmann, R. A., and Amato, R. J. (2008) Exploratory study of  $^{99\text{m}}\text{Tc}$ -EC20 imaging for identifying patients with folate receptor-positive solid tumors. *J. Nucl. Med.* 49, 899–906.
- (10) Leamon, C. P., and Reddy, J. A. (2004) Folate-targeted chemotherapy. *Adv. Drug Delivery Rev.* 56, 1127–1141.
- (11) Li, J., Sausville, E. A., Klein, P. J., Morgenstern, D., Leamon, C. P., Messmann, R. A., and LoRusso, P. (2009) Clinical pharmacokinetics and exposure-toxicity relationship of a folate-vinca alkaloid conjugate EC145 in cancer patients. *J. Clin. Pharmacol.* 49, 1467–1476.
- (12) Konner, J. A., Bell-McGuinn, K. M., Sabbatini, P., Hensley, M. L., Tew, W. P., Pandit-Taskar, N., Els, N. V., Phillips, M. D., Schweizer, C., Weil, S. C., Larson, S. M., and Old, L. J. (2010) Farletuzumab, a humanized monoclonal antibody against folate receptor alpha, in epithelial ovarian cancer: a phase I study. *Clin. Cancer Res.* 16, S288–S295.
- (13) Matteson, E. L., Lowe, V. J., Prendergast, F. G., Crowson, C. S., Moder, K. G., Morgenstern, D. E., Messmann, R. A., and Low, P. S. (2009) Assessment of disease activity in rheumatoid arthritis using a novel folate targeted radiopharmaceutical FolateScan<sup>TM</sup>. *Clin. Exp. Rheum.* 27, 253–259.
- (14) Lu, Y. J., Stinnette, T. W., Westrick, E., Klein, P. J., Gehrke, M. A., Cross, V. A., Vlahov, I. R., Low, P. S., and Leamon, C. P. (2011) Treatment of experimental adjuvant arthritis with a novel folate receptor-targeted folic acid-aminopterin conjugate. *Arthritis Res. Ther.* 13, R56.
- (15) Yi, Y. S., Ayala-Lopez, W., Kularatne, S. A., and Low, P. S. (2009) Folate-targeted hapten immunotherapy of adjuvant-induced arthritis: comparison of hapten potencies. *Mol. Pharmaceutics* 6, 1228–1236.
- (16) Feng, Y., Shen, J. Y., Streaker, E. D., Lockwood, M., Zhu, Z. Y., Low, P. S., and Dimitrov, D. S. (2011) A folate receptor beta-specific

human monoclonal antibody recognizes activated macrophage of rheumatoid patients and mediates antibody-dependent cell-mediated cytotoxicity. *Arthritis Res. Ther.* 13, R59.

(17) Herzog, H. (2001) In vivo functional imaging with SPECT and PET. *Radiochim. Acta* 89, 203–214.

(18) Ametamey, S. M., Honer, M., and Schubiger, P. A. (2008) Molecular imaging with PET. *Chem. Rev.* 108, 1501–1516.

(19) Bettio, A., Honer, M., Müller, C., Brühlmeier, M., Müller, U., Schibli, R., Groehn, V., Schubiger, A. P., and Ametamey, S. M. (2006) Synthesis and preclinical evaluation of a folic acid derivative labeled with  $^{18}\text{F}$  for PET imaging of folate receptor-positive tumors. *J. Nucl. Med.* 47, 1153–1160.

(20) Ross, T. L., Honer, M., Lam, P. Y. H., Mindt, T. L., Groehn, V., Schibli, R., Schubiger, P. A., and Ametamey, S. M. (2008) Fluorine-18 click radiosynthesis and preclinical evaluation of a new  $^{18}\text{F}$ -labeled folic acid derivative. *Bioconjugate Chem.* 19, 2462–2470.

(21) Al Jammaz, I., Al-Otaibi, B., Amer, S., and Okarvi, S. M. (2011) Rapid synthesis and *in vitro* and *in vivo* evaluation of folic acid derivatives labeled with fluorine-18 for PET imaging of folate receptor-positive tumors. *Nucl. Med. Biol.* 38, 1019–1028.

(22) Ross, T. L., Honer, M., Müller, C., Groehn, V., Schibli, R., and Ametamey, S. M. (2010) A new  $^{18}\text{F}$ -labeled folic acid derivative with improved properties for the PET imaging of folate receptor-positive tumors. *J. Nucl. Med.* 51, 1756–1762.

(23) Maschauer, S., and Prante, O. (2009) A series of 2-O-trifluoromethylsulfonyl-D-mannopyranosides as precursors for concomitant  $^{18}\text{F}$ -labeling and glycosylation by click chemistry. *Carbohydr. Res.* 344, 753–761.

(24) Maschauer, S., Einsiedel, J., Haubner, R., Hocke, C., Ocker, M., Hübner, H., Kuwert, T., Gmeiner, P., and Prante, O. (2010) Labeling and glycosylation of peptides using click chemistry: a general approach to  $^{18}\text{F}$ -glycopeptides as effective imaging probes for positron emission tomography. *Angew. Chem., Int. Ed.* 49, 976–979.

(25) Baumann, C. A., Mu, L. J., Wertli, N., Krämer, S. D., Honer, M., Schubiger, P. A., and Ametamey, S. M. (2010) Syntheses and pharmacological characterization of novel thiazole derivatives as potential mGluR5 PET ligands. *Bioorg. Med. Chem.* 18, 6044–6054.

(26) Leamon, C. P., Parker, M. A., Vlahov, I. R., Xu, L. C., Reddy, J. A., Vetzal, M., and Douglas, N. (2002) Synthesis and biological evaluation of EC20: A new folate-derived,  $^{99\text{m}}\text{Tc}$ -based radiopharmaceutical. *Bioconjugate Chem.* 13, 1200–1210.

(27) Reddy, J. A., Xu, L. C., Parker, N., Vetzal, M., and Leamon, C. P. (2004) Preclinical evaluation of  $^{99\text{m}}\text{Tc}$ -EC20 for imaging folate receptor-positive tumors. *J. Nucl. Med.* 45, 857–866.

(28) Honer, M., Brühlmeier, M., Missimer, J., Schubiger, A. P., and Ametamey, S. M. (2004) Dynamic imaging of striatal  $\text{D}_2$ -receptors in mice using quad-HIDAC PET. *J. Nucl. Med.* 45, 464–470.

(29) Mindt, T. L., Müller, C., Melis, M., de Jong, M., and Schibli, R. (2008) “Click-to-Chelate”: In vitro and in vivo comparison of a  $^{99\text{m}}\text{Tc}(\text{CO})_3$ -labeled N( $\tau$ )-histidine folate derivative with its isostructural, clicked 1,2,3-triazole analogue. *Bioconjugate Chem.* 19, 1689–1695.

(30) Müller, C., Reddy, J. A., Leamon, C. P., and Schibli, R. (2010) Effects of the antifolates Pemetrexed and CB3717 on the tissue distribution of  $^{99\text{m}}\text{Tc}$ -EC20 in xenografted and syngeneic tumor-bearing mice. *Mol. Pharmaceutics* 7, 597–604.

(31) Müller, C., Forrer, F., Schibli, R., Krenning, E. P., and de Jong, M. (2008) SPECT study of folate receptor-positive malignant and normal tissues in mice using a novel  $^{99\text{m}}\text{Tc}$ -radiofolate. *J. Nucl. Med.* 49, 310–317.

(32) Hamacher, K., Coenen, H. H., and Stöcklin, G. (1986) Efficient stereospecific synthesis of no-carrier-added 2- $^{18}\text{F}$ -fluoro-2-deoxy-D-glucose using aminopolyether supported nucleophilic substitution. *J. Nucl. Med.* 27, 235–238.

(33) Rostovtsev, V. V., Green, L. G., Fokin, V. V., and Sharpless, K. B. (2002) A stepwise Huisgen cycloaddition process: Copper(I)-catalyzed regioselective “ligation” of azides and terminal alkynes. *Angew. Chem., Int. Ed.* 41, 2596–2599.

(34) Tornøe, C. W., Christensen, C., and Meldal, M. (2002) Peptidotriazoles on solid phase: [1,2,3]-triazoles by regioselective copper(I)-catalyzed 1,3-dipolar cycloadditions of terminal alkynes to azides. *J. Org. Chem.* 67, 3057–3064.

(35) Moses, J. E., and Moorhouse, A. D. (2007) The growing applications of click chemistry. *Chem. Soc. Rev.* 36, 1249–1262.

(36) Müller, C., Mindt, T. L., de Jong, M., and Schibli, R. (2009) Evaluation of a novel radiofolate in tumour-bearing mice: promising prospects for folate-based radionuclide therapy. *Eur. J. Nucl. Med. Mol. Imaging* 36, 938–946.

(37) Goodman, M. M., Elmaleh, D. R., Kearfott, K. J., Ackerman, R. H., Hoop, B., Brownell, G. L., Alpert, N. M., and Strauss, H. W. (1981)  $^{18}\text{F}$ -Labeled 3-deoxy-3-fluoro-D-glucose for the study of regional metabolism in the brain and heart. *J. Nucl. Med.* 22, 138–144.

(38) Czernin, J., Satyamurthy, N., and Schiepers, C. (2010) Molecular mechanisms of bone  $^{18}\text{F}$ -NaF deposition. *J. Nucl. Med.* 51, 1826–1829.

(39) Leamon, C. P., Reddy, J. A., Klein, P. J., Vlahov, I. R., Dorton, R., Bloomfield, A., Nelson, M., Westrick, E., Parker, N., Bruna, K., Vetzal, M., Gehrke, M., Nicoson, J. S., Messmann, R. A., LoRusso, P. M., and Sausville, E. A. (2011) Reducing undesirable hepatic clearance of a tumor-targeted vinca alkaloid via novel saccharopeptidic modifications. *J. Pharmacol. Exp. Ther.* 336, 336–343.